

# Noise from a jet discharging into a duct and its suppression

K.B.M.Q. Zaman<sup>1</sup>, M. M. Clem<sup>2</sup> and A. F. Fagan<sup>3</sup>

NASA Glenn Research Center  
Cleveland, OH 44135

## Abstract

The present study addresses unwanted high intensity noise sometimes encountered in engine test facilities. A simplified model-scale experiment is conducted for a circular jet discharging into a cylindrical duct. For the given configuration the unwanted noise is found to be primarily due to the duct resonance modes excited by the jet. When the ‘preferred mode’ frequency of the jet matches a duct resonant frequency there can be a locked-in ‘super resonance’ accompanied by a high intensity tone. However, even in the absence of a locked-in resonance, high levels of unwanted noise may occur due to the duct modes excited simply by broadband disturbances of the jet. Various methods for suppression of the noise are explored. Tabs placed on the ends of the duct are found ineffective; so are longitudinal fins placed inside the duct. A rod inserted perpendicular to the flow at different axial locations is also found ineffective; however, when there is a super resonance it is effective in suppressing the tone. By far the best suppression is achieved by a wire-mesh screen placed at the downstream end of the duct; placing it on the upstream end also works, however, there is some penalty at high frequencies due to impingement noise. The screen not only eliminates any super resonance but also the duct mode spectral peaks in the absence of such resonance. Apparently it works by dampening the velocity fluctuations at the pressure node and thereby weakening the resonance condition, for the simplified configuration under consideration.

## 1. Introduction

In laboratory tests, sometimes a jet exhaust is dumped into a duct or pipe to route it out of the test chamber, e.g., in large-scale engine tests with hot flows. Occasionally, such a flow precipitates into a resonance-like behavior leading to additional noise. This may obstruct engine noise measurements as well as interfere with flow data. In worst cases, there may be a ‘locked-in’ resonance accompanied by a ‘howl’ that can involve high unsteady aerodynamic loads raising structural concerns. Such phenomena have been encountered historically in different facilities, e.g., at the Arnold Engineering Development Center (AEDC) in the early nineties (see, [1]) as well as in the Propulsion System Laboratory (PSL) at NASA Glenn Research Center (GRC) in 2006. Reference [1] provides a good account of the problem faced at AEDC and also cites similar experiences in a few other facilities in the past. Unfortunately, little documentation can be found for most other cases. The work reported in [1] was followed up by model-scale experiments as well as computational and analytical studies. A 1/48-scale model test at Georgia Institute of Technology as well as a 1/2-scale model test in the PSL at NASA GRC was conducted for the problem faced at one

---

<sup>1</sup> Inlet & Nozzle Branch, Aeropropulsion Division, AIAA Associate Fellow.

<sup>2</sup> Optical Instrumentation Branch, Instrumentation and Controls Division.

<sup>3</sup> Optical Instrumentation Branch, Instrumentation and Controls Division.

of the AEDC facilities ([2], [3]). A general discussion of similar problems experienced with wind tunnels at the Central Aerohydrodynamics Institute (TsAGI) in Russia can be found in [4].

From the literature review, it is apparent that an understanding of the mechanisms of the unwanted noise in test facilities is far from complete. Basically, instability characteristics of the jet exhaust and the acoustic resonance characteristics of the duct/collector come into play. When there is a confluence of the two (i.e., matching of the frequencies and wavenumbers) there can be a coupling leading to sharp resonance, referred to as ‘super resonance’ in [5]. The problem is likely to be akin to such phenomena as ‘whistles’, ring-tones, etc. (e.g., [6], [7]). In [1], with unsteady wall pressure measurements in the duct, for two different nozzle and duct configurations (different facilities within AEDC), it was found that the resonance involved an excitation of the first and second ‘transverse acoustic modes’ (or flapping modes) of the duct. However, the phenomenon is facility and configuration dependent involving a wide range of geometric parameters as well as operating conditions. The duct can be cylindrical, oval or rectangular. It may be of constant diameter or divergent. The nozzle-to-duct diameter ratio as well as stand-off distance may vary. The nozzle geometry dictates the characteristics of the jet plume entering the duct and the flow can be at different Mach numbers and temperatures. Thus, one may not expect that the nature of the excited modes would be the same in all cases. Also, it is possible that a coupling of the jet instability with the duct modes may not be a necessary condition. Simply the excited acoustic modes of the duct by the flow may be enough to raise the noise to unacceptable levels.

As stated already, the phenomenon can hinder aeroacoustic measurements and must be avoided or suppressed. Various methods and modifications of the facilities have been attempted as ‘fixes’. Water spray, Helmholtz resonators, ‘tabs’ (‘dragon teeth’ as referred in [1]), or the protrusion of a rod into the flow (sometimes referred to as a ‘howl stick’) [8], have been used with varying degrees of success. However, as stated in [1], “...these changes have been made on a ‘cut and try’ basis with only limited understanding of the phenomena”. Reference [5] suggested placement of longitudinal fins within the duct with the following rationale. If the excited acoustic modes were spinning or flapping ( $m=\pm 1$ , first helical mode of opposite sense and combination) the expectation was that the fins would retard the azimuthal motion and thus suppress the resonance. However, as stated in the foregoing it is possible that the excited modes may not necessarily be spinning or flapping. The fins may not be effective with the fundamental axisymmetric mode ( $m=0$ ) and its harmonics.

The recurring problem of unwanted noise in test facilities provided the motivation for the present study. The aim was to obtain a better understanding of the aeroacoustic interaction in a simplified, model-scale experiment while trying various methods for suppression of the unwanted noise. As stated before, the investigation so far is limited to a jet from a convergent nozzle discharging into a cylindrical duct with cold subsonic flow. Even in this simplified configuration there is a multitude of variables and thus a parametric study is conducted first to obtain a better understanding of the noise characteristics. Then most of the methods described in the previous paragraph such as tabs, fins and howl stick as well as some new ones are explored in order to suppress the unwanted noise. With the given configuration, while some of the methods are found ineffective and some made matters worse, some did show good promise for suppression. These results are presented in this paper.

## 2. Experimental Facility and Procedure

The experiments are conducted in a small open jet facility at NASA GRC (Fig. 1a). Compressed air passes through a plenum chamber and then exhausts through a convergent nozzle. For all data reported in this paper the nozzle used is a convergent one with diameter,  $d=0.58''$ ; (unless stated otherwise all dimensions are given in inches). A straight pipe section (referred hereafter as ‘duct’) is placed in the jet’s path aligned with its axis. The duct is mounted on a 3-axis traversing mechanism that enables manual positioning in lateral directions and computer controlled positioning in the streamwise direction. The standoff distance from the exit of the nozzle to the entrance of the duct is denoted as  $s$  (see Fig. 1b). Ducts of various diameter ( $D$ ) and length ( $L$ ) are considered;  $D$  is varied as 1'', 1.4'', 2'', 3'' and 4'', and  $L$  is varied as 2'', 3'', 5'', 7'' and 9''; (the mid-ranges of these parameters together with the given nozzle approximates the scales of the configuration in PSL that produced unwanted noise in 2006). The effect of two triangular shaped tabs, each 0.6'' wide at base and 0.5'' high, are tested for suppression of the resonance (Fig. 1c). The tabs could be placed at any desired location within the duct. Wire-mesh screens of two mesh sizes, 16 and 70 per inch, as shown in Fig. 1(d) and (e), are explored. The openness ratio for the two are 51% and 30%, respectively. Figure 1(f) shows a 70-mesh screen with eight  $\frac{1}{4}''$  holes punched on the periphery; the rationale for trying such configuration is explained later. The effect of a cylindrical rod (‘howl stick’) inserted perpendicular to the flow at different locations in the flow path was explored. The rod diameter was chosen to be approximately 10% of the duct diameter after some trials. It was inserted up to the flow axis and could be placed midway between the nozzle and the duct or within the duct at three locations. The latter locations, as indicated in Fig. 1(b), are approximately  $0.2D$  from the ends and at mid-length of the duct. In addition, the effect of three longitudinal fins (Fig. 1d) is also explored with the  $D \times L = 1'' \times 2''$  duct (producing super resonance) following the suggestion in [5]. The fins were 0.625'' long and 0.25'' high and they were placed on the downstream end of the duct. The fins were aligned with the flow and spaced equally in the azimuthal direction.

Sound pressure level measurements were made with a  $\frac{1}{4}$ -inch microphone held fixed at 31'' away from the nozzle exit and placed perpendicular to the jet’s axis. A PC-based data system with ‘LabVIEW’ software was used for all data acquisition and analysis. Spectrum data were acquired using 1000-line analysis over 0-10kHz (i.e., band width=10Hz). The averaging was performed for an ensemble of 100 sample functions taken over a period of 25 seconds. The jet Mach number  $M_j$  was calculated from the ratio of the plenum-to-ambient pressures using isentropic flow equations. All data presented in the following are for ‘cold’ flow, i.e., with total temperature the same everywhere as in the ambient (about 70° F). Jet Mach number  $M_j$  is varied from low subsonic to just over unity.

## 3. Results

Figure 2 shows sound pressure level (SPL) spectra for four different lengths of the duct compared to the free jet case. The jet Mach number  $M_j$  is about 0.46 in all cases. The diameter of the duct is 2'' and the length is varied as 3'', 5'', 7'' and 9'';  $D \times L$  values are indicated in the first column of the legend. The duct standoff distance  $s$  (nondimensionalized by the jet diameter  $d$ ) is shown in the second column,  $M_j$  in the third, and the overall sound pressure level (OASPL, dB) is shown in the last column of the legend. The spectral traces are staggered successively by 1 major ordinate division for easy identification. The trace for the free jet (at the bottom of the figure) is not smooth and ‘peaky’ apparently due to rig noise expected at the low  $M_j$  under consideration. There is a peak around 3.8 kHz and its harmonic that persist in the rest of the spectra in the figure. The important observation is that insertion of the duct in the jet’s path results in a conspicuous peak on the low frequency end. The frequency of this peak decreases with increasing

duct length; the frequencies are about 1650, 1100, 820 and 710 Hz for  $L=3''$ ,  $5''$ ,  $7''$  and  $9''$ , respectively. The estimated half-wave acoustic resonances ( $m=0$  mode) for a duct open on both ends are 1890, 1215, 895 and 710 Hz, respectively for the same four cases [9]. An end correction of  $0.29D$  has been used for the estimates and it can be seen that there are deviations. The end correction deviates more with smaller  $L/D$ . It should also be borne in mind that there is flow through the duct whereas the predicted frequencies are based on resonance involving zero Mach number and feedback with acoustic speed. However, the frequencies are close enough to the prediction and the trend with varying length is right leaving little doubt that these are due to the fundamental half-wave resonance of the duct.

The effect of standoff distance  $s$  for the  $2'' \times 7''$  duct is shown by the spectral traces in Fig. 3; these data are also for  $M_j \approx 0.46$ . As in Fig. 2, the normalized standoff distance is indicated in the second column of the legend. The overall shape of the spectra change very little with varying  $s$  and the peak due to half-wave duct resonance clearly dominates the data. A vertical line is drawn to emphasize that the frequency of the peak does not change perceptibly. Even with variation of  $M_j$  the frequency of the spectral peak changes little. This is shown in Fig. 4; the value of  $M_j$  is indicated in the third column of the legend. However, with increasing  $M_j$  the OASPL (4<sup>th</sup> column in legend) has increased as expected. The spectral peak has broadened somewhat but is still distinguishable at the highest  $M_j$  of 0.87 covered in the figure.

The effect of varying the duct diameter for a fixed length ( $L=7''$ ) is shown in Fig. 5;  $D$  is varied as  $1''$ ,  $1.4''$ ,  $2''$ ,  $3''$  and  $4''$ . A vertical line is drawn through the peak of the spectra for the  $2'' \times 7''$  case. Here, the frequency of the peak shifts perceptibly with varying diameter. The frequency is the lowest with the largest diameter duct. This is expected since with the end correction the effective length is the largest for the largest diameter case. Once again, the end correction of  $0.29D$  does not predict the frequency well for the larger  $D$  (smaller  $L/D$ ) cases. Here, it should be noted that the jet ‘preferred mode’ frequency (assuming a Strouhal number,  $fd/U_j \approx 0.3$ ) is disparately larger than the spectral peak frequencies seen in Figs. 2-5. For example, at  $M_j=0.46$  it is about 3.2 kHz compared to approximately 820 Hz seen in these figures. Thus, the spectral peaks in these figures are not due to a coupling of the jet instability with the duct mode but simply due to an excitation of the duct mode by the broadband disturbances of the flow. It is possible that the unwanted noise encountered in some test facilities is caused by similar duct modes without a coupled super resonance. The super resonance in the present configuration is discussed shortly.

First, the effect of various noise suppression devices on the spectral peaks seen so far is considered. The effect of two tabs (Fig. 1c) is shown in Fig. 6. The red (solid) line is for the baseline (no tab) case; the green (dashed) line and the blue (long-dashed) line are for the effect of the tabs when placed at the downstream and the upstream end of the duct, respectively. It is obvious that there is no perceptible effect of the tabs on the spectra. In the present experiment various other locations of the tabs, e.g., midway and one-quarter way into the duct were also tried with essentially no change in the spectra.

The effect of the ‘howl stick’, in this case a  $0.19''$  diameter rod, is shown in Fig. 7. The three pairs of spectral traces are staggered by a major ordinate division. In each pair the baseline case (denoted ‘bsln’) is repeated. The pair at the bottom compares the effect of the rod when inserted through port 1 in the duct (Fig. 1b). The pair in the middle is for the effect when port 2 is used and the pair at top when the rod is placed between the nozzle and the duct. It can be seen that the spectral peak is not affected significantly. For all cases the rod increases the broadband levels at higher frequencies due to impingement noise. Thus, the rod is ineffective in suppressing the excited duct modes seen in Figs 2-5. Later on, it will be shown that the rod is quite effective in suppressing the resonance due to the coupling of jet instability and the duct mode. The effect of the longitudinal fins for such a resonance condition is also discussed later.

The wire-mesh screens produced tangible suppression of the spectral peaks. Figure 8 shows the effect of the three screen configurations of Figs. 1(d)-(f), when placed on the downstream end of the 2"x7" duct. The data are presented in a manner similar to that in Fig. 7. The effect of the 16-mesh, 70-mesh and the 70-mesh screen with holes is shown successively by the three pairs of traces, the 16-mesh case being at the bottom. The latter case has produced only marginal effect; the OASPL has reduced by 1.3 dB. With the 70-mesh screen there is a clear decrease in the amplitude of the spectral peak. Here the OASPL has decreased by 6 dB. With the fundamental half-wave resonance there is a pressure node (and thus acoustic velocity anti-node) at the ends of the duct. The acoustic velocity fluctuation is likely to be larger in the central portion of the cross-section of the duct and diminish to zero at the wall. Thus, with the assumption of a thick 'boundary layer', an obstruction in the central portion might be expected to be more effective in suppressing the velocity fluctuation and hence the spectral peak. This could be the reason why the tabs did not work since most of the blockage by the tab is at the periphery of the cross-section near the wall. This rationale led to the configuration of Fig. 1(f) with the thought that the holes near the periphery of the cross-section should not diminish the effect too much while reducing the overall blockage to the flow. The pair of spectral traces at the top of Fig. 8 shows the effect for this screen case. It can be seen that the suppression of the spectral peak is not as much as with the full screen case; the decrease in OASPL is 4.1 dB as opposed to 6 dB. Another experiment was conducted with a larger central hole in the 70-mesh screen (hole area same as that of eight 1/4" holes). The difference in the result was minimal (spectra not shown for brevity); the OASPL reduction with the larger hole was only slightly less than that with the eight smaller holes. It is possible that the total blockage might be the key factor dictating the effect but the issue has remained inconclusive. Note that with the tabs the area blockage was only about 10% whereas that with the 70-mesh screen it was 70%.

Since the half-wave resonance involves a velocity anti-node on either end of the duct, the obstruction by the screen on either end should be effective in reducing the resonance. However, when placed on the upstream end there is an increase in broadband noise due to the impingement of the jet (with higher velocity at the upstream location). This is shown in Fig. 9; the effects of the 16-mesh and the 70-mesh screen are shown relative to the no-screen case. These data can be compared with corresponding data in Fig. 8. Compare for example the pair at the top in Fig. 9 with the pair in the middle of Fig. 8 for the effect of the 70-mesh screen. The larger increase in the broadband levels at high frequencies is readily noticeable in Fig. 9. However, it is apparent that the decrease in low frequency noise is more when the screen is placed upstream. The increase in high frequency noise nevertheless dominates the effect and the reduction in OASPL is only 2.2 dB compared to 6dB obtained with the screen placed downstream. Thus, the preferred location of the screen or similar device for suppressing the half-wave resonance should be the downstream end of the duct.

The effect of the 70-mesh screen (placed on downstream end) at three standoff distances ( $s$ ) is compared in Fig. 10. In all cases the spectral peak amplitude is effectively reduced. However, with  $s=0$  the broadband levels have increased significantly at high frequencies, perhaps because the screen is closer to the nozzle and impingement noise is higher. The OASPL reduction is 4.0, 6.3 and 4.3 dB for  $s=0, 3$  and  $5$ , respectively. (The pair of curves for  $s=3$  is slightly different from corresponding data in Fig. 8 as these data were taken in separate batches). Figure 11 shows that the 70-mesh screen is effective in suppressing the spectral peak at other  $M_j$ . However, with increasing  $M_j$  the penalty on the high frequency end is more. The reduction in OASPL at  $M_j = 0.37, 0.69$  and  $0.87$  are 5.9, 4.1 and 2.4 dB, respectively. The variations in the OASPL for the 2"x7" duct with the 16-mesh and the 70-mesh screens are shown in Fig. 12 as a function of  $M_j$ . Both screens are effective throughout the  $M_j$  range covered, the finer mesh screen being

more effective. Also, the effectiveness is more pronounced at low subsonic conditions but diminishes as supersonic conditions are approached.

The data so far show that the duct acoustic modes can be excited by the jet yielding prominent spectral peaks especially at the fundamental half-wave resonance condition. However, a locked-in resonance yielding sharp tones did not take place. As stated in section 1, this can happen when there is an overlap of jet instability frequencies with the duct resonance frequencies. A simple estimate assuming a jet 'preferred mode' Strouhal number of about 0.3 shows that such a condition will be met as  $L/d$  approaches  $1/(0.6M_j)$ . With  $M_j=0.46$ , one would need a duct of about 2" length. However, the jet preferred frequency is not sharply defined and there is a range of velocity over which the coupling condition may be met. Similarly, the end correction for the duct is not rigid and it may be possible to excite the half-wave resonance over a range of frequencies. Recalling that  $L/D$  should not be too small so that the pipe section behaves like a 'duct', three specimens of dimensions 1"x2", 1"x3" and 1.4"x3" were tried. When placed with  $s=0$ , all of them resulted in a sharp resonance with loud tones. The resonances with the 1"x2" duct were the sharpest and data for only this case are considered in the following.

Figure 13 shows SPL spectra for various  $M_j$  for the 1"x2" duct. A sharp spike can be seen in all traces. There is a staging behavior and the frequency of the spike in each stage increases with increasing  $M_j$ . Consider the spectra for  $M_j=0.297$ . The jet 'preferred mode' frequency is about 2100 Hz. The fundamental half-wave resonant frequency with  $0.29D$  end correction is about 2600Hz. In the spectra there are two spikes at about 2 and 3 kHz. Even though the amplitude at 3kHz is larger, it is possible that the one at 2kHz is due to the half-wave resonance coupling with the jet preferred frequency. With slight increase in velocity the lower frequency spike becomes dominant while the one at higher frequency disappears, i.e., there is a stage jump; (note that only limited number of spectral traces are shown in Fig. 13). Between  $M_j=0.416$  and  $0.531$  there is another jump. At  $M_j=0.531$ , there is still a broad peak around 2.8kHz (from the previous stage at lower  $M_j$ ) but the jet preferred frequency is higher which apparently has locked on to another mode of the duct. With further increase in  $M_j$ , the frequency of the spectral spike increases in order to adjust to the increasing frequency of the jet preferred mode. This provides a qualitative explanation of the overall trend. Here, it is worth noting that the 'cut-on' frequency for the first helical mode is calculated to be about 4 kHz, for low Mach number within the duct. With increasing Mach number the cut on frequency decreases. Thus, with increasing  $M_j$  it is possible that higher duct modes cut in and resonate with the jet preferred frequency. However, the details of the duct modes corresponding to the various spikes in Fig. 13 have remained far from clearly understood.

The frequencies of the prominent spectral spikes for the 1"x2" duct are plotted in Fig. 14 as a function of  $M_j$ . These data were acquired by incrementally increasing the jet velocity while monitoring the spectra. Three stages are seen. The stage with the circular data points is apparently due to the half-wave resonance ( $m=0$  fundamental) mode. The nature of the modes in the other two stages remains unclear. In any case, each data point in this figure represents a prominent spike in the spectra corresponding to a locked-in super resonance. As noted earlier, the frequency of the spike in each stage increases with increasing  $M_j$ ; this is apparently dictated by the increase in jet preferred frequency as  $M_j$  is increased. The duct mode frequency adjusts to the jet preferred frequency until the latter becomes disparately different when another duct mode locks in and starts to resonate.

The screens were quite effective in suppressing the super resonance. The effect of the 70-mesh screen is illustrated Fig. 15 by the three pairs of data for three  $M_j$ . Since the figure becomes too crowded with the full legend simplified labels are used. In each pair, the solid (red) curve is for the baseline (no-screen)

case and the dotted (blue) curve is for the screen case. The screen, placed on the downstream end of the duct, was provided with four ¼" holes on the periphery. (The holes in this case were deemed necessary since the blockage with the 70-mesh screen for the smaller duct would be too much.) It can be seen that the screen has eliminated the spectral spikes at all  $M_j$ . The 16-mesh screen was also quite effective even though tones of smaller amplitude persisted at some conditions (spectra not shown for brevity). The overall effects of the screens are shown in Fig. 16, with OASPL versus  $M_j$  data, in a similar format as in Fig. 12. The large drop in OASPL by the screens relative to the no-screen case can be seen readily. Up to 25 dB reduction in the OASPL is noted at some conditions. The 16-mesh screen is seen to perform actually better as supersonic conditions are approached.

The effect of the 'howl stick' (in this case a 0.095" diameter rod) for a condition of super resonance is shown in Fig. 17. The three pairs of spectra are for three locations of the rod, compared to the baseline case. Upon scrutiny it can be seen that the sharp spike at about 4.8 kHz is completely eliminated when the rod is inserted through ports 1 and 2 (Fig. 1b). However, the amplitude of the broadband peak around 2.5 kHz is reduced only a little. When inserted through the port on the downstream end (#3) the tone persists and the effect is seen to be minimal; this can be seen from the pair of traces at the top. Finally, the effect of the longitudinal fins is shown in Fig. 18. The spectral traces for four values of  $M_j$  are compared with the baseline (no fin) case. Very little effect of the fins is seen at lower values of  $M_j$ . Assuming that the excited modes are predominantly axisymmetric it is not surprising that the fins have little effect. At the highest  $M_j$  in Fig. 18, however, a low frequency peak around 2 kHz has been suppressed. It remains unclear but this peak could correspond to a spinning mode. Overall, the effect of the fins was minimal. Thus, so far the screens were found to be the most effective in suppressing not only the super resonance but also the excited duct modes at other conditions.

#### 4. Conclusions

A fundamental experimental study is conducted in order to advance the understanding of noise generated by a jet discharging into a duct. The study is prompted by unwanted noise sometimes encountered in engine test facilities. Based on a simplified model-scale configuration, a circular jet discharging into a cylindrical duct, the following observations are made. The source of the unwanted noise appears to be the duct modes excited by the jet. When the 'preferred mode' frequency of the jet matches a duct resonant frequency there can be a locked-in resonance accompanied by high amplitude tone. The data suggest that even in the absence of such super resonance, high level unwanted noise may occur simply due to excitation of the duct modes by broadband disturbances of the jet. Various methods are tried for suppression of the noise. Tabs placed on the face of the duct are found ineffective. So are longitudinal fins placed inside the duct. A rod inserted perpendicular to the flow is also found generally ineffective; however, it is quite effective when there is super resonance. By far the best suppression is achieved by wire-mesh screens placed on the downstream end of the duct. The screen is effective not only to suppress the super resonance but also the duct modes excited by broadband disturbances. Apparently the screen damps out the velocity perturbations at the pressure node (velocity anti-node) associated with half-wave resonance of the duct. This weakens the resonance condition leading to a reduction in the amplitudes of the spectral peaks.

#### Acknowledgement

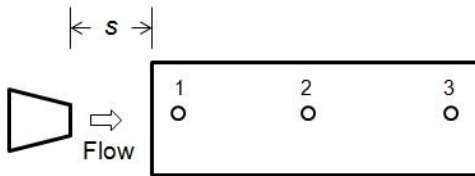
Thanks are due to Dennis L. Huff for helpful comments and suggestions throughout this study. Support from the Supersonics and Subsonic Fixed Wing Projects under NASA's Fundamental Aeronautics Program is gratefully acknowledged.

**References:**

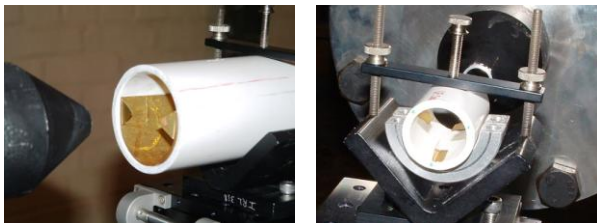
- [1] Jones, R.R. and Lazalier, G.R., “The acoustic response of altitude test facility exhaust systems to axisymmetric and two-dimensional turbine engine exhaust plumes”, DGLR/AIAA Aeroacoustics Conference, Aachen, Germany, Paper 92-02-131, May, 1992.
- [2] Jones, R.R., Ahuja, K.K., Tam, C.K.W. and Abdelwahab, M., “Measured acoustic characteristics of ducted supersonic jets at different model scales”, AIAA Paper 93-0731, 31<sup>st</sup> Aerospace Sciences Meeting, Reno, NV, Jan. 11-14, 1993.
- [3] Tam, C.K.W., Ahuja, K.K. and Jones, R.R., “Screech tones from free and ducted supersonic jets”, AIAA Paper 93-0732, 31<sup>st</sup> Aerospace Sciences Meeting, Reno, NV, Jan. 11-14, 1993.
- [4] Ginevskiy, A.S., Vlasov, Y.V. and Karavosov, R.K., “Acoustic control of turbulent jets”, Springer-Verlag, Berlin, 2004.
- [5] Tam, C.K.W., “Engine test cell aeroacoustics and recommendations”, Final Report, AEDC-TR-06-3, September 30, 2006.
- [6] Nomoto, H. and Culick, F.E.C., “An experimental investigation of pure tone generation by vortex shedding in a duct”, J. Sound & Vib., vol. 84, issue 2, pp. 247-252, 1982.
- [7] Raman, G. and Srinivasan, K., “Whistles: from toys to industrial devices and applications”, Noise Notes, vol. 8, no. 3, July, 2009.
- [8] Kinzie, K.W., “Methods and apparatus for suppressing engine test cell howl”, US Patent no. 6092621, July 25, 2000.
- [9] Stephens, R.W.B. and Bate, A.E., “Acoustics and vibrational physics”, Edward Arnold Publishers Ltd., London, UK, 1966.



(a)



(b)



(c)

(d)



(e)

(f)

(g)

**Fig. 1** Experimental set-up: (a) jet facility with a 2"x7" duct, (b) schematic showing ports for inserting 'howl stick', (c) two tabs placed at upstream end of duct, (d) fins at downstream end of a 1"x2" duct, (e) 16-mesh screen on end, (f) 70-mesh screen, (g) 70-mesh screen with eight 1/4" holes on periphery.

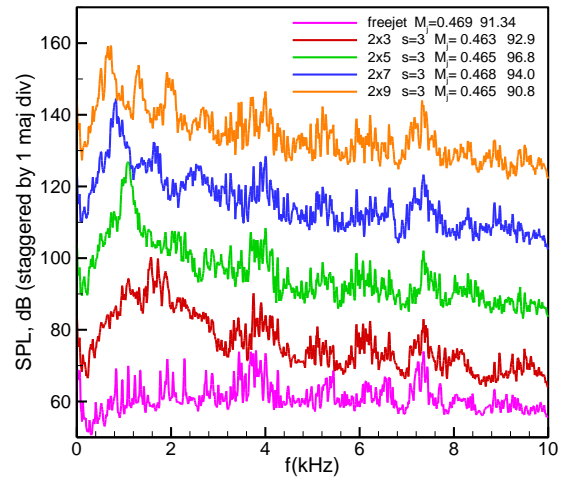


**Fig. 2** SPL spectra for different duct lengths ( $L=3''$ ,  $5''$ ,  $7''$  and  $9''$ ) compared to free jet case;  $D=2''$ ,  $s=3$  ( $s$  is normalized by jet diameter,  $d=0.58''$ ). Jet Mach number ( $M_j$ ) and OASPL (dB) shown in 3rd and 4th columns of legend. Ordinate pertains to curve at bottom; successive curves staggered by one major division.

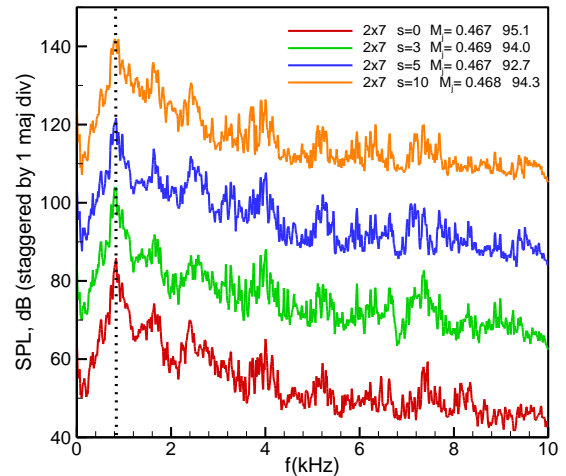


**Fig. 3** SPL spectra for the 2"x7" duct with varying standoff distance ( $s = 0, 3, 5$  and  $10$ );  $M_j \approx 0.47$ .

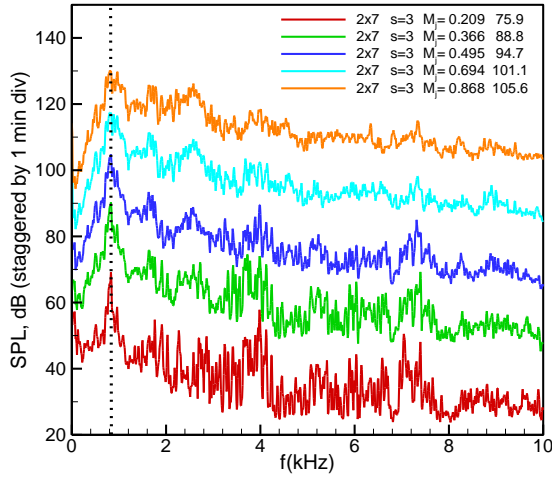


**Fig. 4** SPL spectra for the 2"x7" duct for varying jet Mach number  $M_j$  indicated in the legend;  $s=3$ .

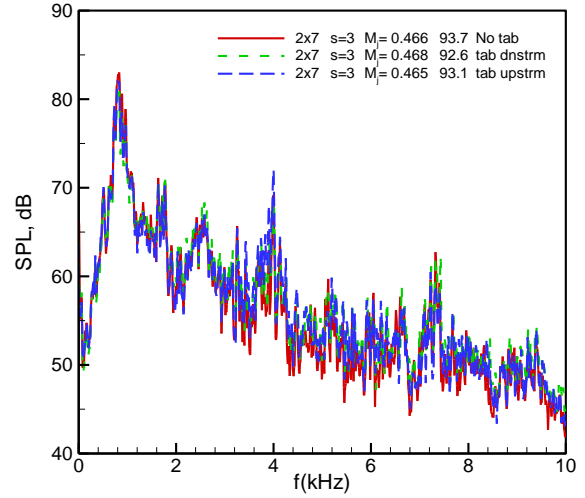


**Fig. 6** Effect of two tabs compared to baseline (No-tab) case. Tabs are placed either downstream or upstream end of duct, as indicated in legend;  $s=3$  and  $M_j \approx 0.47$ .

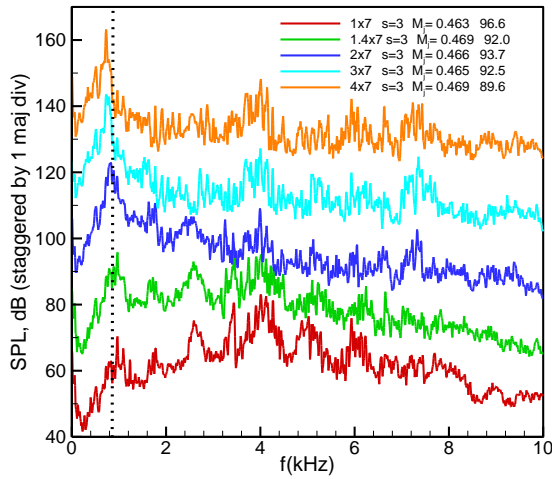


**Fig. 5** SPL spectra for 7" long ducts with varying diameter ( $D=1"$ ,  $1.4"$ ,  $2"$ ,  $3"$  and  $4"$ );  $s=3$ ,  $M_j \approx 0.47$ .

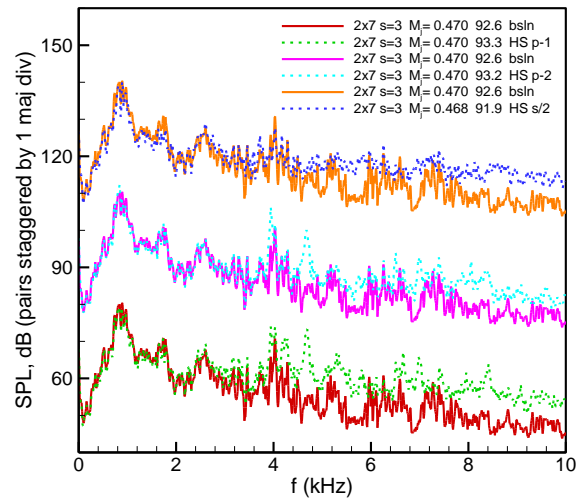


**Fig. 7** Effect of 'howl stick' (0.19" rod) inserted up to about flow centerline for the 2"x7" duct. Port locations shown in Fig. 1(b);  $s=3$ ,  $M_j \approx 0.47$ .

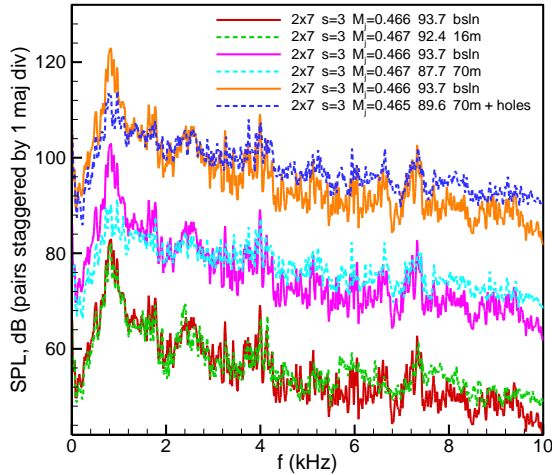


**Fig. 8** Effect of wire-mesh screen placed on downstream end of 2"x7" duct. Pair of curves at bottom compares data for the 16-mesh screen with baseline case ('bsln', no-screen), pair in middle for the 70-mesh screen and pair at top for the 70-mesh screen with holes (see Fig. 1d-f).

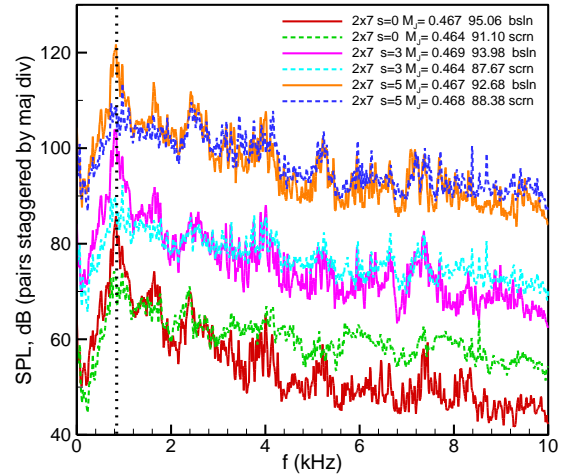


**Fig. 10** Effect of 70-mesh screen (placed on downstream end) of 2"x7" duct relative to baseline case, at different stand-off distance ( $s=0, 3$  and  $5$ ).

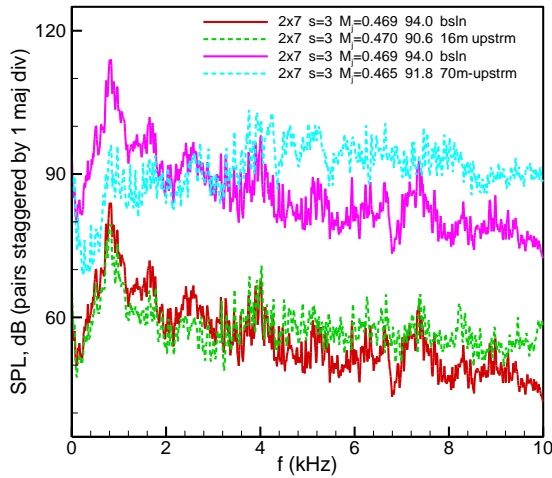


**Fig. 9** Effect of wire-mesh screen placed on upstream end of the 2"x7" duct. Pair of curves at bottom compares data for 16-mesh screen with baseline, pair at top for the 70-mesh screen with baseline.

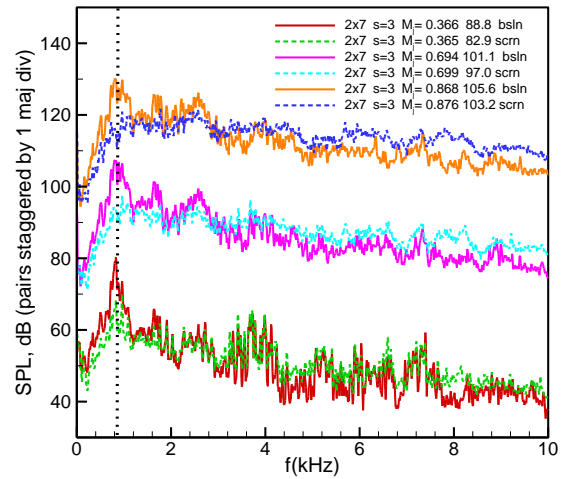


**Fig. 11** Effect of 70-mesh screen placed on downstream end of 2"x7" duct relative to baseline case, at different jet Mach number ( $M_j \approx 0.366, 0.694$  and  $0.868$ ).

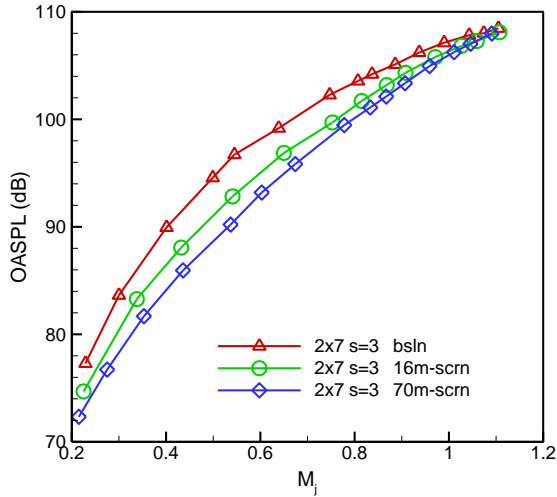


**Fig. 12** Variation of OASPL with  $M_j$  for 2"x7" duct with and without 16- and 70-mesh screens (on the downstream end).

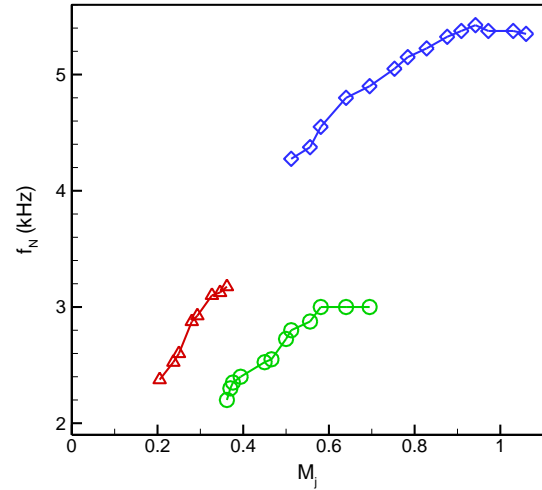


**Fig. 14** Frequency of fundamental tone for the 1"x2" duct as a function of  $M_j$ .

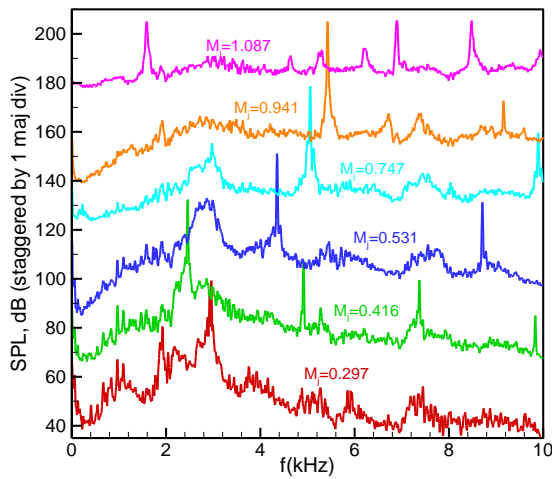


**Fig. 13** SPL spectra for 1"x2" duct producing 'locked-in' resonance. Curves are for different  $M_j$  as indicated;  $s=0$ .

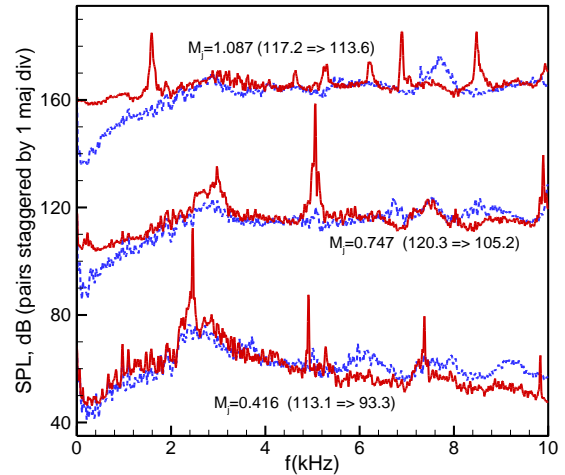


**Fig. 15** SPL spectra showing effect of 70-mesh screen for the 1"x2" duct relative to baseline (no-screen) case. Solid (red) line for baseline, dotted (blue) line for screen (on downstream end). Three pairs of curves are for different  $M_j$  as indicated; change in OASPL indicated in parentheses.

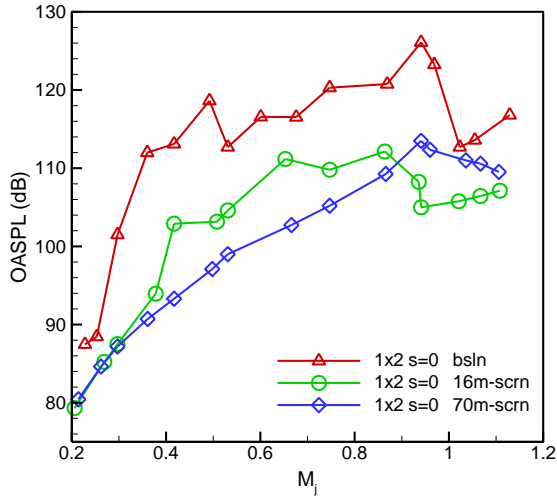


**Fig. 16** Variation of OASPL with  $M_j$  for the 1"x2" duct with and without 16- and 70-mesh screens (on downstream end), shown similarly as in Fig. 12.

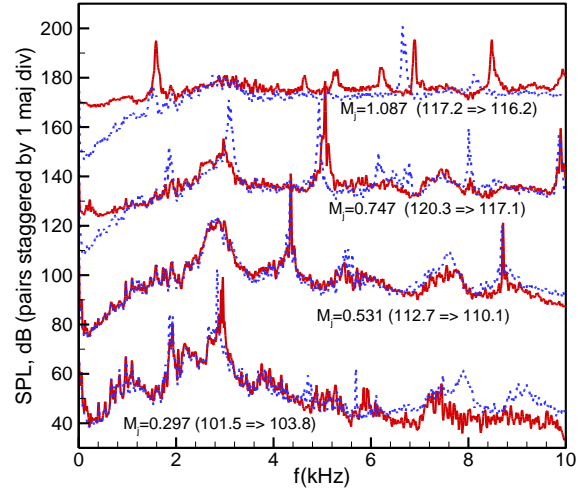


**Fig. 18** Effect of three 1/4"-high longitudinal fins (spaced equally over the periphery at the downstream end) for the 1"x2" duct at four  $M_j$ ;  $s=0$ .

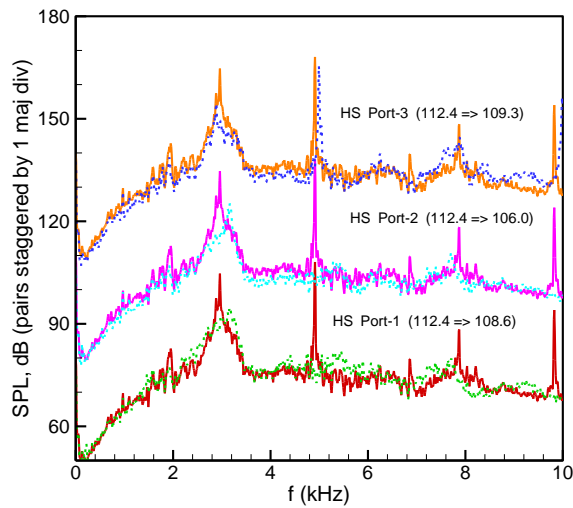


**Fig. 17** Effect of 'howl stick' (0.095" rod inserted up to about flow centerline) for the 1"x2" duct. Port locations shown in Fig. 1(b); changes in OASPL indicated in parentheses;  $s=0$ ,  $M_j \approx 0.67$ .